ACS PHYSICAL CHEMISTRY Au
AN OPEN ACCESS JOURNAL OF THE AMERICAN CHEMICAL SOCIETY

pubs.acs.org/physchemau

Article

Photoelectron Spectroscopy Reveals the Impact of Solvent Additives on Poly(3,4-ethylenedioxythiophene):poly(styrenesulfonate) Thin Film Formation

Yuan Zhang, Qi Wang, Fengyang Hu, Yuhao Wang, Di Wu, Rongbin Wang,* and Steffen Duhm*

Cite This: *ACS Phys. Chem Au* 2023, 3, 311−319

Read Online

ACCESS | Metrics & More | Article Recommendations | Supporting Information

ABSTRACT: The conductive polymer poly(3,4-ethylenedioxythiophene):poly(styrenesulfonate) (PEDOT:PSS) is used in a manifold of electronic applications, and controlling its conductivity is often the key to attain a superior device performance. To that end, solvent additives like Triton, ethylene glycol (EG), or dimethyl sulfoxide (DMSO) are regularly incorporated. In our comprehensive study, we prepare PEDOT:PSS thin films with seven different additive combinations and with thicknesses ranging from 6 to 300 nm on indium-tin-oxide (ITO) substrates. We utilize X-ray photoelectron spectroscopy (XPS) to access the PSS-to-PEDOT ratio and the PSS^--to-PSSH ratio in the near-surface region and ultraviolet photoelectron spectroscopy (UPS) to get the work function (WF). In addition, the morphology and conductivity of these samples are obtained. We found that the WF of the prepared thin films for each combination becomes saturated at a thickness of around 50 nm and thinner films show a lower WF due to the inferior coverage on the ITO. Furthermore, the WF shows a better correlation with the PSS^--to-PSSH ratio than the commonly used PSS-to-PEDOT ratio as PSS^- can directly affect the surface dipole. By adding solvent additives, a dramatic increase in the conductivity is observed for all PEDOT:PSS films, especially when DMSO is involved. Moreover, adding the additive Triton (surfactant) helps to suppress the WF fluctuation for most films of each additive combination and contributes to weaken the surface dipole, eventually leading to a lower and thickness-independent WF.

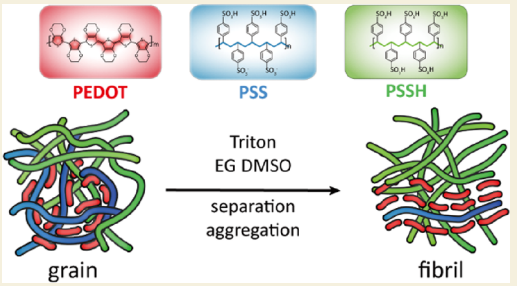

KEYWORDS: *PEDOT:PSS, photoelectron spectroscopy, polar solvents, work function, conductivity*

INTRODUCTION

The conductive polymer poly(3,4-ethylenedioxythiophene):poly(styrenesulfonate) (PEDOT:PSS) finds its application in a plethora of devices, ranging from organic and hybrid organic−inorganic optoelectronic applications[1−5] to biosensors[6,7] and thermoelectric applications.[4,8−10] The wide application of PEDOT:PSS is brought about by its high conductivity, easy accessibility, and low-temperature solution processability.[11−14] The hydrophobic PEDOT is a conjugated polymer and responsible for the high conductivity, whereas insulating hydrophilic PSS acts as a counter ion to stabilize doped PEDOT and to enable the dispersion of PEDOT in water.[15] The structure of PEDOT:PSS can be explained by its conjugated orbitals: some of the C=C double bonds of PEDOT exhibit a benzoid structure as they do in the monomer, which leads to a coil-like macroscopical structure, and the PEDOT-rich core is enclosed by a PSS-rich shell.[16−18]

As shown in Figure 1a, a spatially delocalized π-system is formed along the molecular backbone of PEDOT, while the countercharges are localized on the sulfonate groups of PSS, resulting in the Coulomb interaction between negatively charged monomers on PSS (PSS^-) and PEDOT.[11,15,19] As the pristine PEDOT:PSS shows a core (PEDOT-rich)−shell (PSS-rich) structure in the bulk, excess PSS tends to accumulate close to the surface of the thin films,[20,21] both hindering efficient charge transfer between adjacent PEDOTs and active layers. Thus, numerous efforts have been implemented to optimize the electrical properties of PEDOT:PSS, including changing the configuration of the PEDOT:PSS solution, adding additives, and varying annealing temperature and post-treatment conditions.[22−28] Here, we focus on the discussion about the effect of the additives. Adding additives into to the pristine PEDOT:PSS solution, such as Triton X-100 (Triton or TX), ethylene glycol (EG),

Received: December 13, 2022
Revised: February 1, 2023
Accepted: February 2, 2023
Published: February 20, 2023

https://doi.org/10.1021/acsphyschemau.2c00073
ACS Phys. Chem Au 2023, 3, 311−319

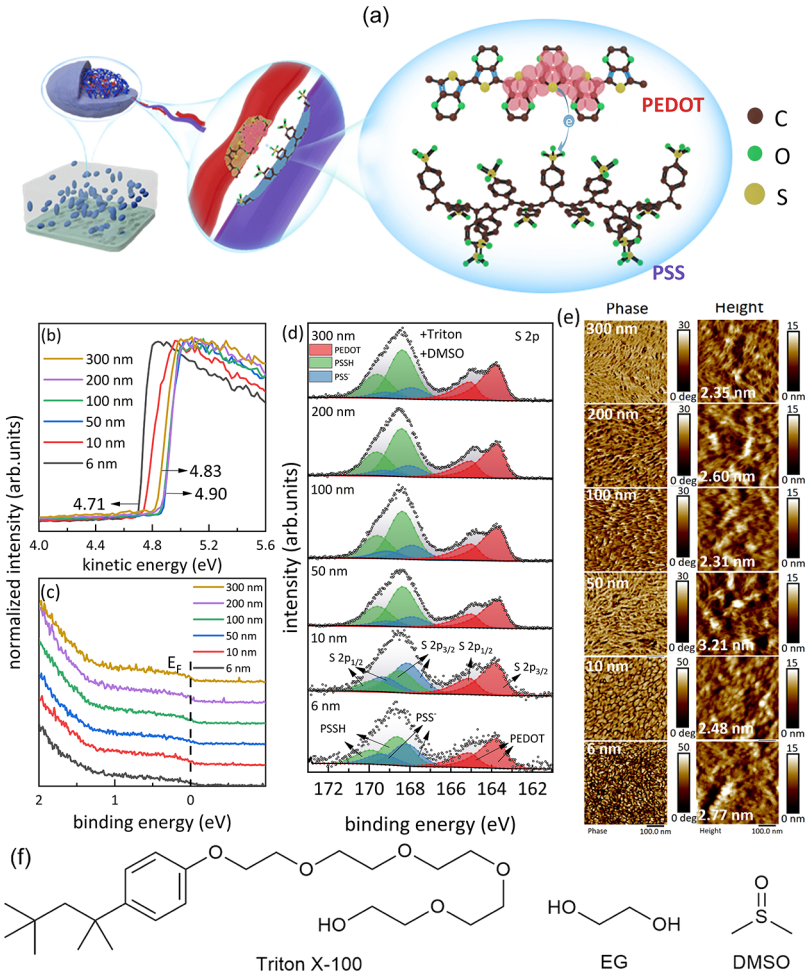

Figure 1. (a) Sketch of a PEDOT:PSS thin film from the macro- to nanoscale. Blue double bonds for benzoid, pink double bonds for quinoid. (b) Secondary electron and (c) valence region of UPS data and (d) XPS-measured S 2p spectra of PEDOT:PSS + Triton + DMSO films with different thicknesses. (e) AFM topography (height and phase, 500 nm × 500 nm) of the same thin films with their respective surface roughness. (f) Chemical structures of Triton X-100, EG, and DMSO.

dimethyl sulfoxide (DMSO) (chemical structures in Figure 1f), or D-sorbitol, is regarded as a convenient approach to bring a higher conductivity by altering the PEDOT:PSS configurations,[29] which is also called "secondary doping". These additives can be roughly divided into "surfactants" and "co-solvents". Apart from being used to adjust the surface tension as the surfactant,[27,30,31] Triton is also beneficial for the conductivity[31] as Triton can combine with both PEDOT and PSS[32,33] and leads to a transformation of the PEDOT C═C double bonds from benzoid to quinoid, which facilitates crystalline packing of PEDOT and elevates the charge transport between PEDOT particles. As mentioned above, PEDOT:PSS comprises PEDOT segments and PSS long chains combined by Coulomb interaction. Some co-solvents can decrease the Coulomb force between PEDOT and PSS and partially release the conducting PEDOT from the surrounding PSS shell. With the help of EG, the PEDOT:PSS morphology changes from core−shell grains into fibrils, and the improved crystallinity together with the PEDOT transformation into quinoid structures contributes to the enhanced carrier mobility and conductivity.[25,34−36] Similar to EG, DMSO also plays a role in improving the electrical properties of PEDOT:PSS by impacting its morphology and chemical composition; furthermore, DMSO can also induce the PSS aggregation and build a bridge effect for charge hopping.[37−40] Despite the successful approaches to modify the PEDOT:PSS films, a unified understanding of the physiochemical mechanisms, which governs the thin film properties, is still missing. For example, it is well-accepted that a PSS-rich surface leads to high WF PEDOT:PSS thin films,[14,41] which was explained by a surface dipole layer formed between PSS and PEDOT.[42,43] However, neutral PSS (PSSH) cannot contribute to a dipole layer and a PSS^--rich surface should be the decisive parameter for work function (WF). Furthermore, PEDOT:PSS thin film properties depend critically on the specifics of thin film preparation (purity of solvents and additives, actual annealing temperature, residual gas in the glove box, etc.), which makes a straightforward comparison of literature results demanding.

In this work, thickness-dependent experiments of PEDOT:PSS films with seven additive combinations have been prepared and characterized by X-ray photoelectron spectroscopy (XPS), ultraviolet photoelectron spectroscopy (UPS), atomic force microscopy (AFM), and four-point probe tests. To figure out the effect of additives in detail, the S 2p and O 1s spectra of PEDOT:PSS thin films with different additives were analyzed to estimate the PEDOT-to-PSS and the PSS^--to-PSSH ratio in the near-surface region to correlate the evolution

https://doi.org/10.1021/acsphyschemau.2c00073
ACS Phys. Chem Au 2023, 3, 311−319

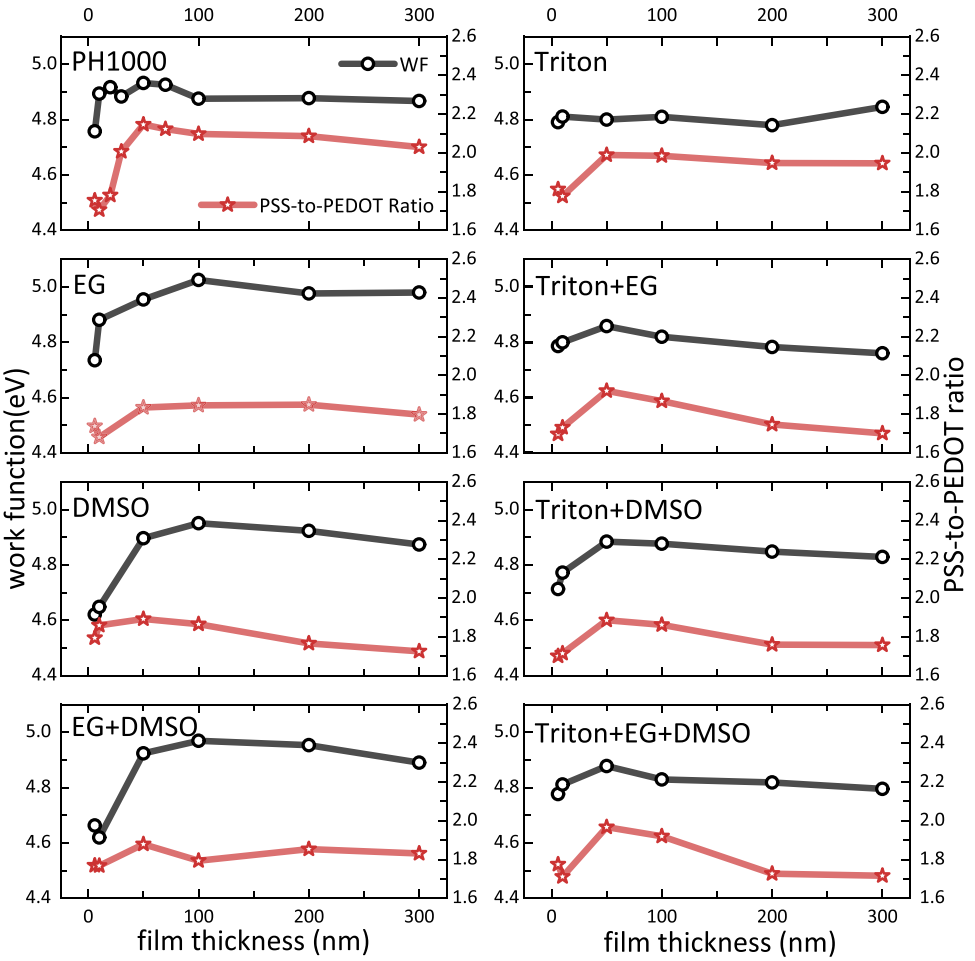

Figure 2. Thickness-dependent work functions and the proportions of PSS to PEDOT obtained from S 2p spectra for PEDOT:PSS films on ITO prepared with different additives.

of the WF of thin films. Based on the AFM analysis and conductivity measurements, a specific illustration of PEDOT:PSS distribution in the surface region is given, which can provide convincing guidance for the application of additive-modified PEDOT:PSS films in optoelectronic devices.

RESULTS

We start with discussing the thickness-dependent electronic and morphological properties of PEDOT:PSS thin films with solvent additives (PH1000 + 1 wt % Triton and + 5 wt % DMSO) optimized for highly conductive layers.[5,44,45] A series of PEDOT:PSS films with different thicknesses (from 6 to 300 nm) were prepared by spin-coating on the ITO substrates (Figure S1), and the processing parameters are given in the Experimental Methods Section. The latent differences for the thick PEDOT:PSS films (≥100 nm) produced by one-step and multi-step spin-coating processes need to be further investigated.

The UPS spectra of the secondary electron cutoff (SECO) and the valence band region are shown in Figure 1b,c, respectively. The WF of the 6 nm-thick PEDOT:PSS films is 4.71 eV and shifts to 4.90 eV as the thickness increases to 50 nm and slightly decreases to 4.83 eV for the 300 nm-thick PEDOT:PSS film. The density of states in the valence electron region close to the Fermi level is almost independent of the film thickness regardless if it is plotted in a linear scale (Figure 1c) or in a semilog scale (Figure S3). The S 2p core-level spectra measured by XPS are shown in Figure 1d. The spectral signatures of PEDOT (at around 164 eV BE) and PSS (at around 169 eV BE) are well separated due to the large chemical shift of the sulfur atoms in the aromatic backbone of PEDOT and the sulfonate groups of PSS.[5,46] To fit the spectra, the S $2p_{1/2}$ and S $2p_{3/2}$ contributions to each S 2p peak have to be considered, as detailed in the Experimental Methods Section. Due to the delocalized π-system of PEDOT, the positive charge density on a particular PEDOT monomer depends on the distance to the PSS^- counter ion, which leads to asymmetric S 2p doublets in the PEDOT contribution.[5,46] In contrast, the charges are localized on PSS^-, leading to two well-separated doublets, which allow the distinction between sulfur atoms in neutral PSSH and in charged PSS^-. The mean free path of the photoelectrons for PEDOT:PSS samples is only about 5−10 nm,[47,48] and the spectra are dominated by the near-surface region. The peak position of the S 2p core level is almost independent of the film thickness. We note that our fitting approach gives a rather robust PSS-to-PEDOT ratio (due to the large chemical shift). However, extracting the PSS^--to-PSSH ratio from the S 2p core-level spectra is more ambiguous and a more straightforward approach is taken by considering the O 1s core levels into account, as detailed further below.

Figure 1e shows the AFM micrographs of the PEDOT:PSS films, and the root mean square (RMS) of the surface roughness decreases from 2.77 to 2.35 nm with increasing

https://doi.org/10.1021/acsphyschemau.2c00073
ACS Phys. Chem Au 2023, 3, 311−319

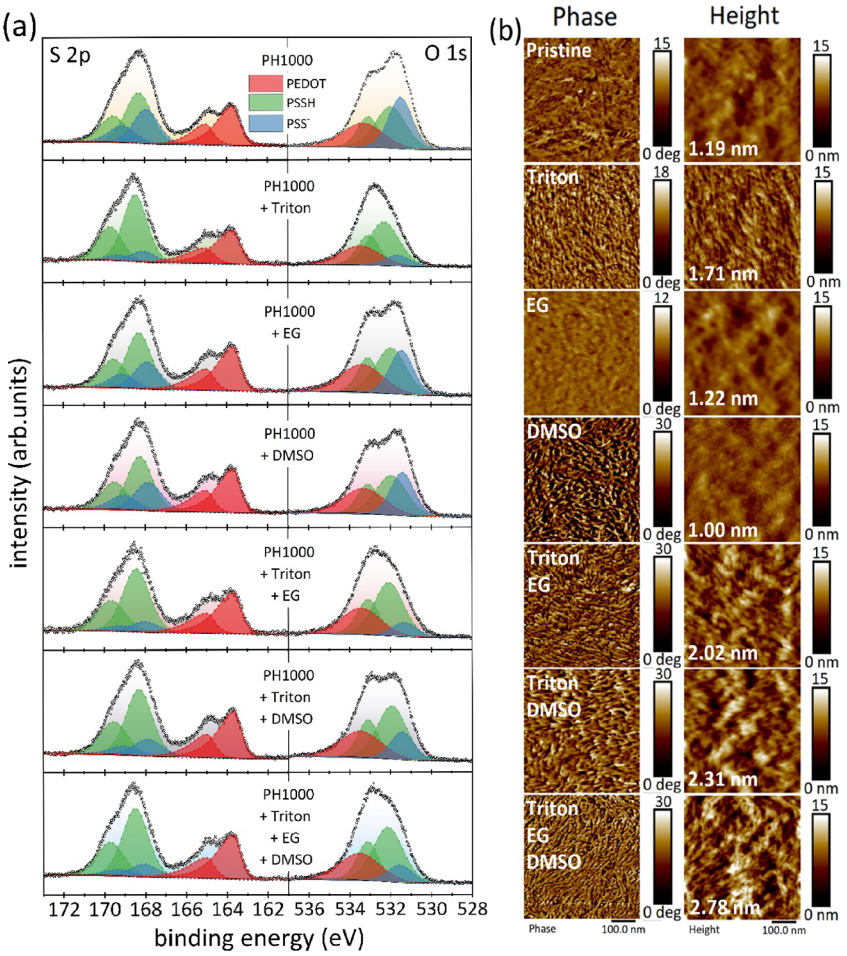

Figure 3. (a) XPS S 2p and O 1s spectra for 100 nm-thick PEDOT:PSS films with different additives. The spectra are fitted into three kinds of chemical states: neutral PSSH (green), charged PSS^- (blue), and PEDOT (red) in which positive charges were delocalized. (b) AFM topography (phase and height, 500 nm × 500 nm) for 100 nm-thick PEDOT:PSS films.

thickness. For ultrathin films (with nominal thicknesses of 6 and 10 nm), the ITO surface is not fully covered, and the granular-like morphology is still impacted by the roughness of the underlying ITO substrate. The phase graph for PEDOT:PSS consists of two different color scales for two phases, a bright area for PEDOT-rich domains and dark area for PSS-rich domains.[14,49,35] Combining the topography from the height and phase graphs, we found that the surface PEDOT:PSS changes from the granular shape for ultrathin films to the fibrillary shape for thicker ones. The AFM results can help to explain the evolution of the WF (Figure 1b): for thinner samples (≤10 nm), the UPS-measured WF is the area-averaged mean WF of covered and uncovered sample patches[50] with a lower WF as the WF of the ITO substrate is only 4.63 eV. For the thicker films (≥50 nm), the substrate is fully covered by PEDOT:PSS and the WF does not show any large variations, which is almost thickness-independent.

To disentangle the effects of the additives (1 wt % Triton; 3 wt % EG; 5 wt % DMSO) on PEDOT:PSS thin film formation, we performed UPS (Figures S2–S5), XPS (Figure S6), and AFM (Figure S7) measurements on thin films with different combinations. The thickness-dependent evolution of the WF (obtained from the UPS SECOs) and the PSS-to-PEDOT ratios (obtained from the area ratios of the respective S 2p spectra) are shown in Figure 2. On the left panel of Figure 2, for the PEDOT:PSS film without any additives (PH1000), the WF shows a slight increase from ultrathin films and saturates at around 4.90 eV for thicknesses larger than 50 nm. Likewise, the PSS-to-PEDOT ratio increases for thicknesses up to 50 nm and then remains relatively stable. The lower WF for thinner layers of pristine PH1000 films can be attributed to the uncovered ITO substrates, as discussed above. The films modified by polar co-solvents without Triton (i.e., EG, DMSO, or EG + DMSO) show a similar trend of the WF evolution but with larger variation from 6 to 100 nm. In contrast, the PSS-to-PEDOT ratios (∼1.8) of these films have almost no thickness-dependent changes and are lower than those of the pristine PH1000 thick films (∼2.0). The results shown here imply that it is not sufficient to explain the evolution of WF of PEDOT:PSS thin films by using the surface PSS-to-PEDOT ratios. Since EG or DMSO can induce phase separation in the solution, excess (free) PSS and PEDOT:PSS complexes coexist in the PEDOT:PSS dispersion;[34,36,39] the lower PSS-to-PEDOT ratio suggests that excess PSS (PSSH) is sufficiently removed during the spin-coating process and not much left on the surface after the thin film formation.

The WF of the films with the surfactant Triton (right panel of Figure 2) as the sole additive is almost thickness-independent, and the PSS-to-PEDOT ratio slightly changes for the lower thicknesses. Triton can induce a phase separation of PEDOT:PSS (with Triton–PEDOT and Triton–PSS complexes) by forming hydrogen bonds.[32,33,51] However, the

https://doi.org/10.1021/acsphyschemau.2c00073
ACS Phys. Chem Au 2023, 3, 311–319

PSS-to-PEDOT ratio is larger than that of the EG- or DMSO-modified films, which suggests that the excess PSS with Triton-PSS complexes are present in the thin films. With the combination of surfactant and polar co-solvents (Triton + EG, Triton + DMSO, and Triton + EG + DMSO), the WFs become thickness-independent again. The constant WFs, compared with the large variation of WFs of EG/DMSO films, are attributed to the superior wetting ability of the surfactant Triton, which leads to the formation of uniform films even for thinner films.[27,30,31] The lower WF when Triton is added shows good agreement with the reported values[27,52] but still lacks a well-established explanation.

The conductivity of all thin films (Figure S8) increases from 6 to 100 nm (except for pristine PH1000 without any additives) and then saturates, which is similar to the evolution of the WF and the surface composition (Figure 2). Thus, we select 100 nm-thick films to expand our discussion on the effect of the additives. By UPS a slight increase in the density of valence band states near E_F for most additive-added PEDOT:PSS films is observed when compared with the pristine 100 nm PEDOT:PSS film (Figure S4). Apart from fitting the S 2p spectra to get the PSS-to-PEDOT ratio, we also included the O 1s core levels (Figure 3a) in the analysis of XPS data to get a more reliable PSS^--to-PSSH ratio. While all oxygen atoms in PEDOT and in PSS^- are in the same respective chemical environment, an additional chemical shift (of around 1.1. eV) takes place between the oxygen atom in the hydroxyl group and the other two oxygen atoms in the sulfonate group of PSSH.[46] All additives reduce the PSS^- contribution to the spectra compared to the pristine PEDOT:PSS film, and the Triton-modified film shows the lowest PSS^- content. Moreover, Triton increases the surface roughness of all PEDOT:PSS films (Figure 3b), while EG or DMSO alone does not notably affect the surface roughness. The AFM phase images reveal that the addition of Triton transforms the grain-like particles into small rod-like ones and modifies the disorganized surface to form some oriented domains, corresponding to the report that Triton can induce the phase separation of PEDOT:PSS grains.[31,32,34] Similarly, by adding EG or DMSO, the particles in the films become enlarged and distinguishable; especially in the DMSO-modified one, the particles are rod-like and more oriented than the Triton-modified ones. In addition, the combination of surfactant Triton and co-solvents EG/DMSO leads to the morphological changes to fibril-like. The high RMS of fibrillary films (Triton + EG, Triton + DMSO, and Triton + EG + DMSO) can be attributed to the morphological transformation from the randomized domain with granular structures to the oriented domain with enlarged fibrillary structures, in which PSS and PEDOT are highly separated and aggregated.[35−38] Due to the close packing of PEDOT and the aggregation of PSS, the surface morphology becomes more oriented but also the surface roughness increases.

DISCUSSION

The summarized WF, PSS-to-PEDOT ratio, PSS^--to-PSSH ratio, and conductivity of the 100 nm thin film for each combination (as shown in Figure 3) are presented in Figure 4, along with the graphical descriptions on how additives impact the surface region of PEDOT:PSS films. It can be clearly distinguished that the WF and the PSS^--to-PSSH ratio show a good correlation, while the PSS-to-PEDOT ratio does not show an obvious evolution tendency with the WF. Compared

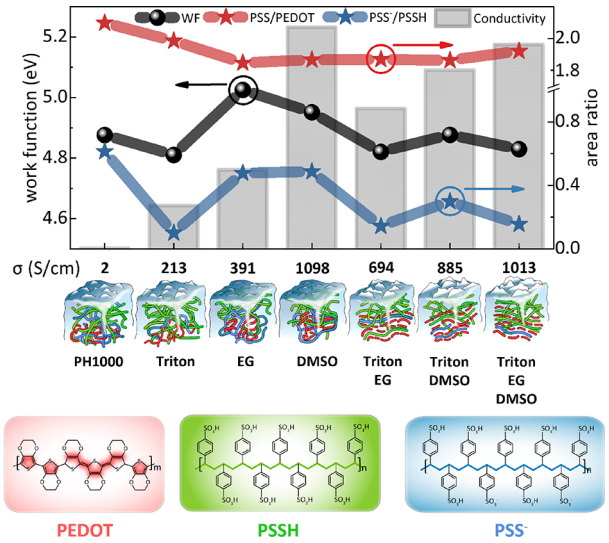

Figure 4. Work functions (from UPS SECOs, Figure S2), PSS-to-PEDOT and PSS^--to-PSSH ratios (from XPS data, Figure 3), and conductivities (Figure S8) of 100 nm-thick PEDOT:PSS films with different solvent additives. The sketches in the middle panel are based on the XPS and AFM data (Figure 3).

with the pristine film, the PSS-to-PEDOT ratio decreases and the conductivity increases when additives are added, which is consistent with previous reports.[16,53] The PEDOT:PSS thin film with DMSO as a sole additive has the highest conductivity and the lowest surface roughness. The very low conductivity of the reference PH1000 film is due to the random distribution of the PEDOT grains, which are separated by surrounding PSS^- and PSSH, leading to low intergrains tunneling or hopping rates.[16,36,40,54] Furthermore, the hydrogen bonds between adjacent PSS long chains and the ionic interaction between PEDOT and PSS make the grains coil-like.[37,55]

With Triton added into the solution, the lowest PSS^--to-PSSH ratio also reduces the WF to the lowest 4.81 eV, corresponding to the induced phase separation of PEDOT:PSS and the resulting decrease in PSS^- amount.[56] Such a large degree of phase separation can be attributed to the long structure of Triton itself and the multiple oxygen and hydrogen sites for the formation of hydrogen bonds, for which the ionic interacted PEDOT and PSS can be pushed away from each other.[33] The overlapped region of PEDOT increases, which improves the conductivity to 212 S/cm. However, the conductivity is still inferior due to the distortion of $\pi-\pi$ stacking, for which the quinoid structure will turn back to benzoid or an intermediate structure, thus the lower carrier mobility.[37] Compared with Triton, EG and DMSO show a stronger effect to remove excess PSS (PSSH) and leave more PSS^- on the surface, leading to the higher WFs (5.03 eV for EG, 4.95 eV for DMSO). Though EG and DMSO have a similar impact on the PSS^--to-PSSH ratio, compared with EG, particles in the DMSO-modified film are more ordered, as shown in the phase graph in Figure 3b, resulting in the highest conductivity. The priority of DMSO in particle realignment can be attributed to the superior effect of DMSO on the formation of PSS segregations. The improvement of conductivity for EG/DMSO additives can be attributed to the enhanced carrier mobility resulting from the decreased excess PSS barrier.[25,34,39,57]

https://doi.org/10.1021/acsphyschemau.2c00073
ACS Phys. Chem Au 2023, 3, 311−319

In the PEDOT:PSS films with multiple additives, the addition of Triton can decrease the PSS^--to-PSSH ratio compared with that of only EG or DMSO participation, thus decreasing the WF. In addition, the synergy of Triton with EG, DMSO, or EG + DMSO can boost the transformation of the granular structures into fibrillary ones, as shown in Figure 3b. Therefore, the charge hopping barrier can be lowered, which improves the conductivity. The films modified with Triton + DMSO are found to keep more PSS^- inside the film compared to the films modified with other combinations of surfactants and polar co-solvents, which can be regarded as the reason of the larger variation of the WFs of corresponding films. The increase in the PSS^- content can be explained by the proton transfer or proton sharing effect wherein DMSO interacts strongly with PSSH by forming hydrogen bonding with short bond length and PSSH would share the proton with DMSO, which leads to the formation of deprotonated PSS^- anions.[58] When EG is further appended into the same solution, the proton sharing effect of DMSO becomes weakened, leading to the decrease in PSS^--to-PSSH ratio in Triton + EG + DMSO-modified films. The decrease in PSS^- composition in the surface region contributes to the low WF, which is also the reason why, in comparison with the films without Triton, the WFs of these films with Triton are almost independent of the film thickness (Figure 2). Overall, the PSS^--to-PSSH ratio can govern the surface dipole and consequently the WF of the thin film. The electrical improvement is the synergy of the modified fibrillary structure (the crystallinity), the decreased PSS barrier between the conducting PEDOT grains (the carrier mobility in the charge hopping mechanism), and the ratio of the quinoid structure.

CONCLUSIONS

Our work illustrates that 100 nm is a proper thickness for additive-modified spin-coated PEDOT:PSS films to obtain a saturated conductivity and clearly demonstrates the spatial distribution and morphological transformation of additive-modified PEDOT:PSS in the surface region. The surfactant Triton not only adjusts the surface tension to form a uniform film but also can decrease the WF by impacting the ratio of PSS^- to PSSH as it has more capability to remove the surface PSS^-. EG and DMSO show the similar effect on excess PSS removal, but DMSO has the potential to transform the PSSH into PSS^- by the proton sharing effect. Most importantly, the additives tune the WF by changing the PSS^--to-PSSH ratio, which directly contributes to the surface dipole. More PSS^- inside can lead to the larger variation of WF with thickness increasing. All the additives have the ability to improve the conductivity by removing the insulating barrier caused by excess PSS and increasing the crystallinity by forming a fibril film. The highest conductivity is contributed by the 100 nm-thick DMSO-modified film, which is 1098.2 S/cm.

EXPERIMENTAL METHODS

Materials and Substrate Preparation

PEDOT:PSS solution (Clevios PH1000 with a PEDOT-to-PSS mass ratio of 1:2.5) was purchased from Heraeus. Triton X-100 and ethylene glycol (EG) were purchased from Innochem, and dimethyl sulfoxide (DMSO) was purchased from J&K. The substrates—ITO (SKJYLEAN, Suzhou Suke lean instrument Co. LTD) and silicon with an oxide layer (30 nm)—were cut into 1 cm × 1 cm squares. To ensure the similar film-forming properties, all the substrates were ultrasonically cleaned in acetone, methanol, and deionized (DI) water for 20 min, followed by UV-ozone treatment for 20 min to remove insoluble contaminants, forming the hydrogen bonds on the surface.

PEDOT:PSS Film Preparation

The precursor solution PH1000 was mixed with different additives (1 wt % Triton X-100 for the wetting agent, 3 wt % EG and 5 wt % DMSO for co-solvents), and the mixed solutions were diluted with different proportions of DI water such as 1:0.5, 1:1, 1:1.5, and 1:3 (mixture/water volume ratio). All the diluted solutions were blended for 5 min by a vortex mixer before being used. To prevent the substrates from turning hydrophobic after air exposure, PEDOT:PSS films were prepared by spin-coating once the substrates had been cleaned and transferred into an N_2-filled glove box. Thicker films were prepared by spin coating multiple times after 5 min of drying for each layer. After spin-coating, all the samples were annealed at 125 °C for 20 min in the glove box.

Characterization

The surface morphology was measured by atomic force microscopy (AFM, by Veeco.). The film thickness of thinner films (6−50 nm) was measured by spectroscopic ellipsometry (SE, by J.A. Woollam Co., Inc.), while the thickness of thicker films (50−300 nm) was confirmed by measuring the steps of tweezer scratches using AFM. A four-point probe tester was used to measure the conductivity of PEDOT:PSS films on SiO_2 substrates. XPS (Al Kα, 1486.74 eV) and UPS (He Iα, 21.22 eV) measurements were carried out with monochromatized light sources in a customized SPECS photoelectron spectroscopy system[59] including an analysis chamber (base pressure: 3×10^{-10} mbar) and a sample load-lock. All the samples were prepared and annealed in a N_2-filled glove box and finally transferred into an analysis chamber with a N_2-filled load lock to protect the samples from air exposure and air degradation. All measurements were carried out at room temperature (295 K). The secondary electron spectra were plotted as a function of kinetic energy corrected by the applied bias voltage (−3 V) and the analyzer WF. In such a way, the position of the SECO corresponded to the position of VL above E_F.[60] The core-level spectra were fitted by a convolution of Voigt peaks with a Shirley background using CasaXPS. For fitting the S 2p-derived peaks, the relative intensity of S $2p_{1/2}$ and S $2p_{3/2}$ was fixed to 1:2 and the splitting energy to 1.18 eV. The S 2p doublets contributed from PEDOT were fitted with an asymmetric line shape LF(1,4,5,0) in CasaXPS.

ASSOCIATED CONTENT

Supporting Information

The Supporting Information is available free of charge at https://pubs.acs.org/doi/10.1021/acsphyschemau.2c00073.

Thickness configuration work of PEDOT:PSS films (Figure S1), UPS SECOs and valence band regions of PEDOT:PSS films (Figures S2−S5); XPS spectra of the S 2p core level from PEDOT:PSS films on ITO (Figure S6); AFM height images of PEDOT:PSS layers on ITO (Figures S7), and conductivity of PEDOT:PSS films measured using the four-point probe tester (Figures S8) (PDF)

AUTHOR INFORMATION

Corresponding Authors

Rongbin Wang − *Institut für Physik and IRIS Adlershof, Humboldt-Universität zu Berlin, 12489 Berlin, Germany;* orcid.org/0000-0001-6094-4028; Email: rongbin@physik.hu-berlin.de

Steffen Duhm − *Institute of Functional Nano & Soft Materials (FUNSOM), Joint International Research Laboratory of Carbon-Based Functional Materials and Devices and Jiangsu Key Laboratory of Advanced Negative*

https://doi.org/10.1021/acsphyschemau.2c00073
ACS Phys. Chem Au 2023, 3, 311−319

Carbon Technologies, Soochow University, Suzhou 215123, People's Republic of China; orcid.org/0000-0002-5099-5929; Email: duhm@suda.edu.cn

Authors

Yuan Zhang − *Institute of Functional Nano & Soft Materials (FUNSOM), Joint International Research Laboratory of Carbon-Based Functional Materials and Devices and Jiangsu Key Laboratory of Advanced Negative Carbon Technologies, Soochow University, Suzhou 215123, People's Republic of China*

Qi Wang − *Institute of Functional Nano & Soft Materials (FUNSOM), Joint International Research Laboratory of Carbon-Based Functional Materials and Devices and Jiangsu Key Laboratory of Advanced Negative Carbon Technologies, Soochow University, Suzhou 215123, People's Republic of China;* orcid.org/0000-0002-9777-3637

Fengyang Hu − *Institute of Functional Nano & Soft Materials (FUNSOM), Joint International Research Laboratory of Carbon-Based Functional Materials and Devices and Jiangsu Key Laboratory of Advanced Negative Carbon Technologies, Soochow University, Suzhou 215123, People's Republic of China*

Yuhao Wang − *Institute of Functional Nano & Soft Materials (FUNSOM), Joint International Research Laboratory of Carbon-Based Functional Materials and Devices and Jiangsu Key Laboratory of Advanced Negative Carbon Technologies, Soochow University, Suzhou 215123, People's Republic of China*

Di Wu − *Institute of Functional Nano & Soft Materials (FUNSOM), Joint International Research Laboratory of Carbon-Based Functional Materials and Devices and Jiangsu Key Laboratory of Advanced Negative Carbon Technologies, Soochow University, Suzhou 215123, People's Republic of China*

Complete contact information is available at: https://pubs.acs.org/10.1021/acsphyschemau.2c00073

Author Contributions

CRediT: **Yuan Zhang** conceptualization (equal), formal analysis (lead), investigation (lead), writing-original draft (lead); **Qi Wang** formal analysis (supporting), funding acquisition (supporting), investigation (supporting), supervision (supporting), writing-review & editing (supporting); **Fengyang Hu** formal analysis (supporting), investigation (supporting); **Yuhao Wang** formal analysis (supporting), investigation (supporting); **Di Wu** formal analysis (supporting), investigation (supporting); **Rongbin Wang** conceptualization (lead), formal analysis (supporting), funding acquisition (supporting), supervision (supporting), writing-review & editing (equal); **Steffen Duhm** conceptualization (equal), funding acquisition (lead), resources (lead), supervision (lead), writing-review & editing (lead).

Notes

The authors declare no competing financial interest.

ACKNOWLEDGMENTS

Financial support from the National Natural Science Foundation of China (Grant No. 22150610468), the Collaborative Innovation Center of Suzhou Nano Science & Technology (NANO-CIC), the 111 Project of the Chinese State Administration of Foreign Experts Affairs, the Suzhou Key Laboratory of Functional Nano & Soft Materials, and the Deutsche Forschungsgemeinschaft (DFG), Project number SFB951-182087777, are gratefully acknowledged.

REFERENCES

(1) Fagiolari, L.; Varaia, E.; Mariotti, N.; Bonomo, M.; Barolo, C.; Bella, F. Poly(3,4-ethylenedioxythiophene) in Dye-Sensitized Solar Cells: Toward Solid-State and Platinum-Free Photovoltaics. *Adv. Sustainable Syst.* **2021**, *5*, 2100025.

(2) Liu, L.; Wu, L.; Yang, H.; Ge, H.; Xie, J.; Cao, K.; Cheng, G.; Chen, S. Conductivity and Stability Enhancement of PEDOT:PSS Electrodes *via* Facile Doping of Sodium 3-Methylsalicylate for Highly Efficient Flexible Organic Light-Emitting Diodes. *ACS Appl. Mater. Interfaces* **2022**, *14*, 1615−1625.

(3) Pei, S.; Xiong, X.; Zhong, W.; Xue, X.; Zhang, M.; Hao, T.; Zhang, Y.; Liu, F.; Zhu, L. Highly Efficient Organic Solar Cells Enabled by the Incorporation of a Sulfonated Graphene Doped PEDOT:PSS Interlayer. *ACS Appl. Mater. Interfaces* **2022**, *14*, 34814−34821.

(4) Wu, X.; Tang, X.; Dong, X.; Jiang, Z.; Liu, N.; Bao, J.; Cui, G.; Zhao, C.; Kong, L.; Gu, M. Improving the Electrical Properties and Hole Extraction Efficiency of Inverted Perovskite Solar Cells with $AuCl_3$ Interfacial Modification Layer. *Phys. Status Solidi A* **2022**, *219*, 2200163.

(5) Wang, R.; Wang, Y.; Wu, C.; Zhai, T.; Yang, J.; Sun, B.; Duhm, S.; Koch, N. Direct Observation of Conductive Polymer Induced Inversion Layer in N-Si and Correlation to Solar Cell Performance. *Adv. Funct. Mater.* **2020**, *30*, 1903440.

(6) Zeng, R.; Wang, W.; Chen, M.; Wan, Q.; Wang, C.; Knopp, D.; Tang, D. CRISPR-Cas12a-Driven MXene-PEDOT:PSS Piezoresistive Wireless Biosensor. *Nano Energy* **2021**, *82*, No. 105711.

(7) Gupta, S.; Datt, R.; Mishra, A.; Tsoi, W. C.; Patra, A.; Bober, P. Poly(3,4-ethylenedioxythiophene):Poly(Styrene Sulfonate) in Antibacterial, Tissue Engineering and Biosensors Applications: Progress, Challenges and Perspectives. *J. Appl. Polym. Sci.* **2022**, *139*, No. e52663.

(8) Liu, L.; Chen, J.; Liang, L.; Deng, L.; Chen, G. A PEDOT:PSS Thermoelectric Fiber Generator. *Nano Energy* **2022**, *102*, No. 107678.

(9) Wang, J.; Li, Q.; Li, K.; Sun, X.; Wang, Y.; Zhuang, T.; Yan, J.; Wang, H. Ultra-High Electrical Conductivity in Filler-Free Polymeric Hydrogels Toward Thermoelectrics and Electromagnetic Interference Shielding. *Adv. Mater.* **2022**, *34*, 2109904.

(10) He, X.; Gu, J.; Hao, Y.; Zheng, M.; Wang, L.; Yu, J.; Qin, X. Continuous Manufacture of Stretchable and Integratable Thermoelectric Nanofiber Yarn for Human Body Energy Harvesting and Self-Powered Motion Detection. *Chem. Eng. J.* **2022**, *450*, No. 137937.

(11) Elschner, A.; Kirchmeyer, S.; Lovenich, W.; Merker, U.; Reuter, K. *PEDOT: Principles and Applications of an Intrinsically Conductive Polymer*, 0 ed.; CRC Press, 2010, DOI: 10.1201/b10318.

(12) Zhan, C.; Yu, G.; Lu, Y.; Wang, L.; Wujcik, E.; Wei, S. Conductive Polymer Nanocomposites: A Critical Review of Modern Advanced Devices. *J. Mater. Chem. C* **2017**, *5*, 1569−1585.

(13) Kayser, L. V.; Lipomi, D. J. Stretchable Conductive Polymers and Composites Based on PEDOT and PEDOT:PSS. *Adv. Mater.* **2019**, *31*, 1806133.

(14) Fan, X.; Nie, W.; Tsai, H.; Wang, N.; Huang, H.; Cheng, Y.; Wen, R.; Ma, L.; Yan, F.; Xia, Y. PEDOT:PSS for Flexible and Stretchable Electronics: Modifications, Strategies, and Applications. *Adv. Sci.* **2019**, *6*, 1900813.

(15) Groenendaal, L.; Jonas, F.; Freitag, D.; Pielartzik, H.; Reynolds, J. R. Poly(3,4-Ethylenedioxythiophene) and Its Derivatives: Past, Present, and Future. *Adv. Mater.* **2000**, *12*, 481−494.

(16) Jönsson, S. K. M.; Birgerson, J.; Crispin, X.; Greczynski, G.; Osikowicz, W.; Denier van der Gon, A. W.; Salaneck, W. R.; Fahlman, M. The Effects of Solvents on the Morphology and Sheet Resistance in Poly(3,4-Ethylenedioxythiophene)−Polystyrenesulfonic Acid (PEDOT−PSS) Films. *Synth. Met.* **2003**, *139*, 1−10.

(17) Kirchmeyer, S.; Reuter, K. Scientific Importance, Properties and Growing Applications of Poly(3,4-Ethylenedioxythiophene). *J. Mater. Chem.* **2005**, *15*, 2077.
(18) Crispin, X.; Marciniak, S.; Osikowicz, W.; Zotti, G.; van der Gon, A. W. D.; Louwet, F.; Fahlman, M.; Groenendaal, L.; De Schryver, F.; Salaneck, W. R. Conductivity, Morphology, Interfacial Chemistry, and Stability of Poly(3,4-Ethylene Dioxythiophene)-Poly(Styrene Sulfonate): A Photoelectron Spectroscopy Study. *J. Polym. Sci., Part B: Polym. Phys.* **2003**, *41*, 2561−2583.
(19) Mikhnenko, O. V.; Blom, P. W. M.; Nguyen, T.-Q. Exciton Diffusion in Organic Semiconductors. *Energy Environ. Sci.* **2015**, *8*, 1867−1888.
(20) Yun, D.; Jung, J.; Sung, Y. M.; Ra, H.; Kim, J.; Chung, J.; Kim, S. Y.; Kim, Y.; Heo, S.; Kim, K.; Jeong, Y. J.; Jang, J. In-Situ Photoelectron Spectroscopy Study on the Air Degradation of PEDOT:PSS in Terms of Electrical and Thermoelectric Properties. *Adv. Electron. Mater.* **2020**, *6*, 2000620.
(21) Hwang, J.; Amy, F.; Kahn, A. Spectroscopic Study on Sputtered PEDOT·PSS: Role of Surface PSS Layer. *Org. Electron.* **2006**, *7*, 387−396.
(22) Nardes, A. M.; Kemerink, M.; de Kok, M. M.; Vinken, E.; Maturova, K.; Janssen, R. A. J. Conductivity, Work Function, and Environmental Stability of PEDOT:PSS Thin Films Treated with Sorbitol. *Org. Electron.* **2008**, *9*, 727−734.
(23) Huang, J.; Miller, P. F.; Wilson, J. S.; de Mello, A. J.; de Mello, J. C.; Bradley, D. D. C. Investigation of the Effects of Doping and Post-Deposition Treatments on the Conductivity, Morphology, and Work Function of Poly(3,4-Ethylenedioxythiophene)/Poly(Styrene Sulfonate) Films. *Adv. Funct. Mater.* **2005**, *15*, 290−296.
(24) Friedel, B.; Keivanidis, P. E.; Brenner, T. J. K.; Abrusci, A.; McNeill, C. R.; Friend, R. H.; Greenham, N. C. Effects of Layer Thickness and Annealing of PEDOT:PSS Layers in Organic Photodetectors. *Macromolecules* **2009**, *42*, 6741−6747.
(25) Wei, Q.; Mukaida, M.; Naitoh, Y.; Ishida, T. Morphological Change and Mobility Enhancement in PEDOT:PSS by Adding Co-Solvents. *Adv. Mater.* **2013**, *25*, 2831−2836.
(26) Wang, X.; Liu, P.; Jiang, Q.; Zhou, W.; Xu, J.; Liu, J.; Jia, Y.; Duan, X.; Liu, Y.; Du, Y.; Jiang, F. Efficient DMSO-Vapor Annealing for Enhancing Thermoelectric Performance of PEDOT:PSS-Based Aerogel. *ACS Appl. Mater. Interfaces* **2019**, *11*, 2408−2417.
(27) Zhou, X.; Dong, X.; Liu, Y.; Wang, W.; Wei, W.; Chen, J.; Liu, T.; Zhou, Y. Effect of Wetting Surfactants on the Work Function of PEDOT:PSS for Organic Solar Cells. *ACS Appl. Energy Mater.* **2022**, *5*, 3766−3772.
(28) Wu, D.; Wan, S.; Zhai, T.; Yang, J.; Wang, R.; Duhm, S. Impact of Substrate Hydrophobicity on Layer Composition and Work Function of PEDOT:PSS Thin Films. *Phys. Status Solidi RRL* **2022**, *16*, 2100434.
(29) Modarresi, M.; Zozoulenko, I. Why Does Solvent Treatment Increase the Conductivity of PEDOT: PSS? Insight from Molecular Dynamics Simulations. *Phys. Chem. Chem. Phys.* **2022**, *24*, 22073−22082.
(30) Cinquino, M.; Prontera, C. T.; Zizzari, A.; Giuri, A.; Pugliese, M.; Giannuzzi, R.; Monteduro, A. G.; Carugati, M.; Banfi, A.; Carallo, S.; Rizzo, A.; Andretta, A.; Dugnani, G.; Gigli, G.; Maiorano, V. Effect of Surface Tension and Drying Time on Inkjet-Printed PEDOT:PSS for ITO-Free OLED Devices. *J. Sci.* **2022**, *7*, 100394.
(31) Oh, J. Y.; Shin, M.; Lee, J. B.; Ahn, J.-H.; Baik, H. K.; Jeong, U. Effect of PEDOT Nanofibril Networks on the Conductivity, Flexibility, and Coatability of PEDOT:PSS Films. *ACS Appl. Mater. Interfaces* **2014**, *6*, 6954−6961.
(32) Yoon, S.-S.; Khang, D.-Y. Roles of Nonionic Surfactant Additives in PEDOT:PSS Thin Films. *J. Phys. Chem. C* **2016**, *120*, 29525−29532.
(33) Kim, S.; Lee, S. J.; Cho, S.; Shin, S.; Jeong, U.; Myoung, J.-M. Improved Stability of Transparent PEDOT:PSS/Ag Nanowire Hybrid Electrodes by Using Non-Ionic Surfactants. *Chem. Commun.* **2017**, *53*, 8292−8295.
(34) Kim, Y. H.; Sachse, C.; Machala, M. L.; May, C.; Müller-Meskamp, L.; Leo, K. Highly Conductive PEDOT:PSS Electrode with Optimized Solvent and Thermal Post-Treatment for ITO-Free Organic Solar Cells. *Adv. Funct. Mater.* **2011**, *21*, 1076−1081.
(35) Thomas, J. P.; Leung, K. T. Mixed Co-Solvent Engineering of PEDOT:PSS to Enhance Its Conductivity and Hybrid Solar Cell Properties. *J. Mater. Chem. A* **2016**, *4*, 17537−17542.
(36) Alemu Mengistie, D.; Wang, P.-C.; Chu, C.-W. Effect of Molecular Weight of Additives on the Conductivity of PEDOT:PSS and Efficiency for ITO-Free Organic Solar Cells. *J. Mater. Chem. A* **2013**, *1*, 9907.
(37) Yu, L.-M.; Chen, T.; Feng, N.; Wang, R.; Sun, T.; Zhou, Y.; Wang, H.; Yang, Y.; Lu, Z.-H. Highly Conductive and Wettable PEDOT:PSS for Simple and Efficient Organic/C-Si Planar Heterojunction Solar Cells. *Sol. RRL* **2020**, *4*, 1900513.
(38) Thomas, J. P.; Zhao, L.; McGillivray, D.; Leung, K. T. High-Efficiency Hybrid Solar Cells by Nanostructural Modification in PEDOT:PSS with Co-Solvent Addition. *J. Mater. Chem. A* **2014**, *2*, 2383.
(39) Lee, I.; Kim, G. W.; Yang, M.; Kim, T.-S. Simultaneously Enhancing the Cohesion and Electrical Conductivity of PEDOT:PSS Conductive Polymer Films Using DMSO Additives. *ACS Appl. Mater. Interfaces* **2016**, *8*, 302−310.
(40) Pietsch, M.; Bashouti, M. Y.; Christiansen, S. The Role of Hole Transport in Hybrid Inorganic/Organic Silicon/Poly(3,4-Ethylenedioxy-Thiophene):Poly(Styrenesulfonate) Heterojunction Solar Cells. *J. Phys. Chem. C* **2013**, *117*, 9049−9055.
(41) Sun, Z.; He, Y.; Xiong, B.; Chen, S.; Li, M.; Zhou, Y.; Zheng, Y.; Sun, K.; Yang, C. Performance-Enhancing Approaches for PEDOT:PSS-Si Hybrid Solar Cells. *Angew. Chem., Int. Ed.* **2021**, *60*, 5036−5055.
(42) Niederhausen, J.; Mazzio, K. A.; MacQueen, R. W. Inorganic−Organic Interfaces in Hybrid Solar Cells. *Electron. Struct.* **2021**, *3*, No. 033002.
(43) Koch, N.; Vollmer, A.; Elschner, A. Influence of Water on the Work Function of Conducting Poly(3,4-Ethylenedioxythiophene)/Poly(Styrenesulfonate). *Appl. Phys. Lett.* **2007**, *90*, No. 043512.
(44) Yoon, S.-S.; Khang, D.-Y. High Efficiency (>17%) Si-Organic Hybrid Solar Cells by Simultaneous Structural, Electrical, and Interfacial Engineering via Low-Temperature Processes. *Adv. Energy Mater.* **2018**, *8*, 1702655.
(45) Xu, Q.; Song, T.; Cui, W.; Liu, Y.; Xu, W.; Lee, S.-T.; Sun, B. Solution-Processed Highly Conductive PEDOT:PSS/AgNW/GO Transparent Film for Efficient Organic-Si Hybrid Solar Cells. *ACS Appl. Mater. Interfaces* **2015**, *7*, 3272−3279.
(46) Greczynski, G.; Kugler, T.; Salaneck, W. R. Characterization of the PEDOT-PSS System by Means of X-Ray and Ultraviolet Photoelectron Spectroscopy. *Thin Solid Films* **1999**, *354*, 129−135.
(47) Greczynski, G.; Hultman, L. A Step-by-Step Guide to Perform x-Ray Photoelectron Spectroscopy. *J. Appl. Phys.* **2022**, *132*, No. 011101.
(48) Wang, Q.; Yang, J.; Gerlach, A.; Schreiber, F.; Duhm, S. Advanced Characterization of Organic−Metal and Organic−Organic Interfaces: From Photoelectron Spectroscopy Data to Energy-Level Diagrams. *J. Phys. Mater.* **2022**, *5*, No. 044010.
(49) Vosgueritchian, M.; Lipomi, D. J.; Bao, Z. Highly Conductive and Transparent PEDOT:PSS Films with a Fluorosurfactant for Stretchable and Flexible Transparent Electrodes. *Adv. Funct. Mater.* **2012**, *22*, 421−428.
(50) Schultz, T.; Lenz, T.; Kotadiya, N.; Heimel, G.; Glasser, G.; Berger, R.; Blom, P. W. M.; Amsalem, P.; de Leeuw, D. M.; Koch, N. Reliable Work Function Determination of Multicomponent Surfaces and Interfaces: The Role of Electrostatic Potentials in Ultraviolet Photoelectron Spectroscopy. *Adv. Mater. Interfaces* **2017**, *4*, 1700324.
(51) Luo, R.; Li, H.; Du, B.; Zhou, S.; Zhu, Y. A Simple Strategy for High Stretchable, Flexible and Conductive Polymer Films Based on PEDOT:PSS-PDMS Blends. *Org. Electron.* **2020**, *76*, No. 105451.
(52) Shin, D.; Kang, D.; Lee, J.-B.; Ahn, J.-H.; Cho, I.-W.; Ryu, M.-Y.; Cho, S. W.; Jung, N. E.; Lee, H.; Yi, Y. Electronic Structure of

Nonionic Surfactant-Modified PEDOT:PSS and Its Application in Perovskite Solar Cells with Reduced Interface Recombination. *ACS Appl. Mater. Interfaces* **2019**, *11*, 17028−17034.
(53) Choi, S.; Kim, W.; Shin, W.; Han, H. J.; Park, C.; Oh, H.; Jung, S.; Park, S.; Lee, H. Electronic Structure Modification of Polymeric PEDOT:PSS Electrodes Using the Nonionic Surfactant Brij C10 Additive for Significant Sheet Resistance Reduction. *Appl. Surf. Sci.* **2023**, *610*, No. 155609.
(54) Gao, P.; Yang, Z.; He, J.; Yu, J.; Liu, P.; Zhu, J.; Ge, Z.; Ye, J. Dopant-Free and Carrier-Selective Heterocontacts for Silicon Solar Cells: Recent Advances and Perspectives. *Adv. Sci.* **2018**, *5*, 1700547.
(55) Shi, H.; Liu, C.; Jiang, Q.; Xu, J. Effective Approaches to Improve the Electrical Conductivity of PEDOT:PSS: A Review. *Adv. Electron. Mater.* **2015**, *1*, 1500017.
(56) Sakunpongpitiporn, P.; Phasuksom, K.; Paradee, N.; Sirivat, A. Facile Synthesis of Highly Conductive PEDOT:PSS *via* Surfactant Templates. *RSC Adv.* **2022**, *9*, 6363−6378.
(57) Na, S.-I.; Wang, G.; Kim, S.-S.; Kim, T.-W.; Oh, S.-H.; Yu, B.-K.; Lee, T.; Kim, D.-Y. Evolution of Nanomorphology and Anisotropic Conductivity in Solvent-Modified PEDOT:PSS Films for Polymeric Anodes of Polymer Solar Cells. *J. Mater. Chem.* **2009**, *19*, 9045.
(58) Yildirim, E.; Wu, G.; Yong, X.; Tan, T. L.; Zhu, Q.; Xu, J.; Ouyang, J.; Wang, J.-S.; Yang, S.-W. A Theoretical Mechanistic Study on Electrical Conductivity Enhancement of DMSO Treated PEDOT:PSS. *J. Mater. Chem. C* **2018**, *6*, 5122−5131.
(59) Lu, M.-C.; Wang, R.-B.; Yang, A.; Duhm, S. Pentacene on Au(1 1 1), Ag(1 1 1) and Cu(1 1 1): From Physisorption to Chemisorption. *J. Phys.: Condens. Matter* **2016**, *28*, No. 094005.
(60) Schultz, T. A Unified Secondary Electron Cut-off Presentation and Common Mistakes in Photoelectron Spectroscopy. *Electron. Struct.* **2022**, *4*, No. 044002.

https://doi.org/10.1021/acsphyschemau.2c00073
ACS Phys. Chem Au 2023, 3, 311−319